Molecular Interactions Between Sex Hormone-Binding Globulin and Nonsteroidal Ligands That Enhance Androgen Activity

Round, Phillip

2020-01-31

Round , P , Das , S , Wu , T-S , Wähälä , K , Van Petegem , F & Hammond , G 2020 , ' Molecular Interactions Between Sex Hormone-Binding Globulin and Nonsteroidal Ligands That Enhance Androgen Activity ' , Journal of Biological Chemistry , vol. 295 , no. 5 , pp. 1202-1211 . https://doi.org/10.1074/jbc.RA119.011051

http://hdl.handle.net/10138/312591
https://doi.org/10.1074/jbc.RA119.011051

unspecified
publishedVersion

Molecular interactions between sex hormone–binding globulin and nonsteroidal ligands that enhance androgen activity

Received for publication, September 12, 2019, and in revised form, December 16, 2019 Published, Papers in Press, December 18, 2019, DOI 10.1074/jbc.RA119.011051

Phillip Round[‡], Samir Das[§], Tsung-Sheng Wu[‡], Kristiina Wähälä[¶‖], Filip Van Petegem[§], and Geoffrey L. Hammond[‡1]

From the [‡]Department of Cellular & Physiological Sciences and [§]Department of Biochemistry and Molecular Biology, The University of British Columbia, Vancouver, BC Canada V6T 1Z4 and [¶]Department of Biochemistry and Development Biology and [‖]Department of Chemistry, University of Helsinki, Finland 00100

Edited by Joseph M. Jez

Sex hormone–binding globulin (SHBG) determines the equilibrium between free and protein-bound androgens and estrogens in the blood and regulates their access to target tissues. Using crystallographic approaches and radiolabeled competitive binding-capacity assays, we report here how two nonsteroidal compounds bind to human SHBG, and how they influence androgen activity in cell culture. We found that one of these compounds, (−)3,4-divanillyltetrahydrofuran (DVT), present in stinging nettle root extracts and used as a nutraceutical, binds SHBG with relatively low affinity. By contrast, a synthetic compound, 3-(1H-imidazol-1-ylmethyl)-2phenyl-1H-indole (IPI), bound SHBG with an affinity similar to that of testosterone and estradiol. Crystal structures of SHBG in complex with DVT or IPI at 1.71–1.80 Å resolutions revealed their unique orientations in the SHBG ligand-binding pocket and suggested opportunities for the design of other nonsteroidal ligands of SHBG. As observed for estradiol but not testosterone, IPI binding to SHBG was reduced by ∼20-fold in the presence of zinc, whereas DVT binding was almost completely lost. Estradiol-dependent fibulin-2 interactions with SHBG similarly occurred for IPI-bound SHBG, but not with DVT-bound SHBG. Both DVT and IPI increased the activity of testosterone in a cell culture androgen reporter system by competitively displacing testosterone from SHBG. These findings indicate how nonsteroidal ligands of SHBG maybe designed to modulate the bioavailability of sex steroids.

Steroid hormone bioavailability is delineated by the "free hormone hypothesis" and its underlying tenet that steroids only enter cells when they are not bound by plasma proteins (1). Sex hormone–binding globulin (SHBG)[2] is produced by hepatocytes and it binds biologically active androgens and estrogens, thereby regulating their plasma levels and bioavailability (2). Human SHBG is a homodimer, with each monomer comprising two laminin G (LG) domains (3). The N-terminal LG domain contains a steroid-binding site and the dimerization interface (3, 4). The dimerization of SHBG depends on the occupancy of a calcium-binding site within the N-terminal LG domain and dimerization is stabilized by the binding of steroid ligands (5). The carboxyl-terminal LG domain plays no role in steroid binding or dimerization but contains two *N*-linked glycosylation sites, the utilization of which may prolong its plasma half-life (6, 7).

The active androgen, 5α-dihydrotestosterone (DHT), has the highest affinity ∼1 nM K_d for SHBG followed by testosterone and estradiol, which bind with ∼5 and ∼20 times lower affinities, respectively, when compared with DHT (8). Androgens and estrogens are positioned in opposite orientations within the same hydrophobic pocket in crystal structures of the N-terminal LG domain of SHBG such that the steroid ring A of androgens is buried within the protein near Ser-42, whereas the ring D of estrogens resides in this position, and this steroid class–dependent difference in their orientation causes minor structural variation in the protein (9). Notably, a flexible loop region formed by residues 130–135 appears to form a lid over an entrance to the SHBG steroid-binding pocket. This loop region usually appears disordered in crystal structures when androgens are present in the binding site but is more ordered when estradiol is bound so that key residues within it interact with this steroid (9, 10). Occupancy of a zinc-binding site in this region of human SHBG also alters the positioning of this loop region and the binding affinity of estrogens (10–12).

Evidence that this flexible loop region serves as the main portal for sex steroids is largely circumstantial. However, an mAb binds an epitope in this region, and presumably constrains the mobility of the loop, and this appears to prevent the movement of DHT into and out of the steroid-binding site, whereas the binding of estradiol is only marginally affected (13). This led to the suggestion that estradiol has an alternative route of entry into or exit from the steroid-binding site when compared with

This work was supported by the Canadian Institutes of Health Research Grant MOP 15261 (to G. L. H.) and the Canada Research Chair in Reproductive Health Tier 1 (to G. L. H.). The authors declare that they have no conflicts of interest with the contents of this article.

This article contains Fig. S1.

The atomic coordinates and structure factors (codes 6PYF, 6PYB, and 6PYA) have been deposited in the Protein Data Bank (http://wwpdb.org/).

[1] To whom correspondence should be addressed. E-mail: geoffrey.hammond@ubc.ca.

[2] The abbreviations used are: SHBG, sex hormone binding globulin; DHT, 5α-dihydrotestosterone; DVT, (−)3,4-divanillyltetrahydrofuran; IPI, 3-(1H-imidazol-1-ylmethyl)-2phenyl-1H-indole; LG, laminin G; RMSD, root mean square deviation; RBA, relative binding affinity; DCC, dextran-coated charcoal.

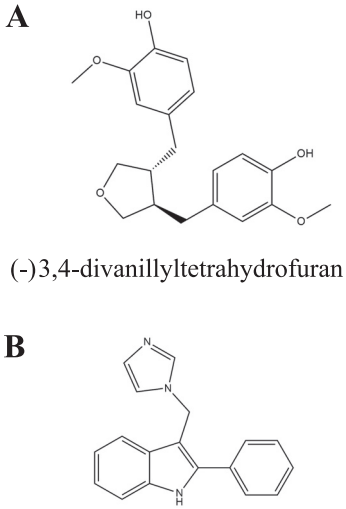

Figure 1. Chemical structures of nonsteroidal ligands of SHBG. *A*, chemical structure of DVT, a plant-derived lignan. *B*, chemical structure of IPI, a synthetic compound provided by Pfizer as a potential SHBG ligand.

DHT (13). If the steroid-binding pocket of SHBG has multiple entrances, it is possible that other lipophilic ligands of SHBG (14) access it differently and reside within it in unique orientations.

Numerous nonsteroidal ligands of SHBG have been identified, including several endocrine disrupting compounds (14, 15). Among these, (−)3,4-divanillyltetrahydrofuran (DVT) is a natural compound present in stinging nettle root extracts used for the treatment of benign prostatic hypertrophy (Fig. 1) (16, 17) and is widely used as a nutraceutical with anabolic properties (18). We therefore set out to determine the molecular interactions between SHBG and DVT, as well as a novel nonsteroidal compound, 3-(1H-imidazol-1-ylmethyl)-2phenyl-1H-indole (IPI) provided by Pfizer (PF-0102478) as a potential SHBG ligand (Fig. 1), and we have studied their ability to displace androgens from SHBG and to enhance their bioavailability.

Results

Crystal structure of SHBG E176K in complex with estradiol

The N-terminal LG domain of human SHBG E176K crystallizes within 24 h into large 3-dimensional diamond-shaped crystals in space group $P4_322$ that provide reliable data collection. The crystal structure of estradiol-bound SHBG E176K was determined at 1.73 Å and solved by molecular replacement with the published N-terminal LG domain SHBG structure in complex with estradiol (9). Data collection parameters and refinement statistics are presented in Table 1. When these structures are superimposed, the steroid-binding pocket, the flexible loop region that covers it, and the position and orientation of estradiol do not differ from each other (Fig. 2*A*). Structural alignment of α carbon atoms between estradiol-bound E176K and previously published estradiol-bound WT SHBG structures resulted in a RMSD of 1.25 Å. Residues involved in steroid binding are positioned as expected (Fig. 2*B*). Although the orientation of Trp-84 differs in position, its electron density in SHBG E176K is poorly defined, indicating that there may be a secondary conformation for this residue. In addition, the side chain of Lys-173 is displaced and a suspected water molecule is organized by hydrogen bonding between Lys-173 and Lys-176, when compared with Glu-176 (Fig. 2*C*), and this change is located near residues (Leu-171–Lys-173) that are displaced when estradiol is bound (10).

Crystal structure of SHBG E176K in complex with DVT

The crystal structure of SHBG E176K in complex with DVT was determined at 1.80 Å and solved by molecular replacement with the estradiol-bound SHBG E176K structure. This shows that DVT is bound at same site as sex steroids but occupies more of the hydrophobic pocket, while maintaining key residue interactions (Fig. 3*A*). No major changes to the globular structure were observed when compared with other SHBG crystal structures with several steroid ligands (Fig. 3*A*) (3, 9, 10). The binding pocket was occupied by DVT in an orientation where vanillyl group A and the THF ring sit in the same position as a steroid, but the second vanillyl group B occupies a volume that is normally empty when a steroid is bound (Fig. 3*A*). This crystal structure implies that Ser-42 contributes significantly to the binding of DVT, as observed for all SHBG ligands (14), but this appears to be mediated through a water molecule that bridges Ser-42 and the oxygen of the THF ring (Fig. 3*B*). The other key interaction is a hydrogen bond between Asp-65 and the hydroxyl group of vanillyl group A that appears to also hold the ligand in place. A less significant contribution to binding is implied for Arg-135, which borders the flexible lidlike loop that is disordered (residues Leu-131–Ser-133) when DVT is bound (Fig. 2*A*). Although Arg-135 reaches into the binding pocket, it is not clear if it hydrogen bonds directly with DVT; instead, it may stabilizes the contact with Asp-65 through an ionic interaction (Fig. 3*B*). The disordering of the loop is caused by DVT displacing Leu-131 and an outward movement and rearrangement of the loop that allows Arg-135 to stabilize DVT binding, and this contrasts with the corresponding role of Lys-134 in estradiol-bound structures (Fig. 3*A*). The positioning of Trp-84, a surface residue near the flexible loop region of SHBG, in the DVT-bound structure mirrors that in the estradiol-bound SHBG structure (9).

Crystal structure of SHBG E176K in complex with IPI

The crystal structure of E176K SHBG in complex with IPI was determined at 1.71 Å and solved by molecular replacement with the SHBG E176K estradiol-bound structure (Fig. 4). No major changes to the globular structure of the protein were noted, whereas structural variation occurred throughout the binding pocket. The binding of IPI was determined by three major interactions involving Ser-42, Phe-67, and Asp-65 (Fig. 3*B*). Serine 42 interacts with the nitrogen of the imidazole portion of IPI through a hydrogen bond of 2.7 Å. Residue Phe-67 π-π stacks with IPI through its phenyl group at a distance of 4 Å. Interestingly, this interaction forces Phe-67 into an alternate conformation as compared with when DVT or steroids are bound (Fig. 4*A*). This conformation of Phe-67 rearranges the hydrophobic binding pocket sufficiently to allow the perpendicular positioning of IPI relative to DHT (Fig. 4*A*), which leaves a large portion of the binding pocket empty in the IPI

Table 1
Data collection and refinement statistics
Statistics for the highest-resolution shell are shown in parentheses. One crystal was used for each dataset.

	E2-bound E176K SHBG	DVT-bound E176K SHBG	IPI-bound E176K SHBG
Data Collection			
Space group	P 43 2 2	P 43 2 2	P 43 2 2
Cell dimensions			
a, b, c (Å)	51.87, 51.87, 149.6	51.95, 51.95, 148.4	52.24, 52.24, 147.9
Total reflections	44,460 (4330)	39,386 (3802)	46,065 (4470)
Unique reflections	22,230 (2165)	19,693 (1901)	23,048 (2235)
Resolution range	42.6–1.73 (1.79–1.73)	29.5–1.80 (1.86–1.80)	25.7–1.71 (1.77–1.71)
R_{merge} (%)	1.3 (18.0)	1.2 (21.0)	1.3 (13.0)
CC1/2	1 (0.929)	1 (0.910)	1 (0.959)
CC*	1 (0.981)	1 (0.976)	1 (0.989)
I/σI	23.0 (4.2)	23.0 (3.1)	24.0 (4.4)
Completeness (%)	99.6 (100)	99.9 (100)	99.7 (100)
Refinement			
Resolution	42.6–1.73 (1.79–1.73)	29.5–1.80 (1.86–1.80)	25.7–1.71 (1.77–1.71)
R_{work}/R_{free} (%)	18.4/22.1	20.3/23.1	18.5/21.6
Number of atoms			
Protein	1395	1356	1412
Ligands	21	26	22
Water	186	110	121
Average B-factors			
Protein	28.2	41.2	32.0
Ligands	19.5	45.8	27.4
Water	34.8	42.8	37.4
RMSD bond lengths (Å)	0.008	0.003	0.006
RMSD bond angles (°)	1.05	0.75	0.84
Ramachandran statistics			
Favored regions (%)	95.9	95.8	97.1
Allowed regions (%)	4.1	4.2	2.9
Outliers (%)	0	0	0
Rotamer outliers (%)	0	0.7	1.3
Clash score	1.07	1.47	2.11
MolProbity score	1.11 (99th percentile of similar resolution structures)	1.20 (99th percentile of similar resolution structures)	1.14 (99th percentile of similar resolution structures)

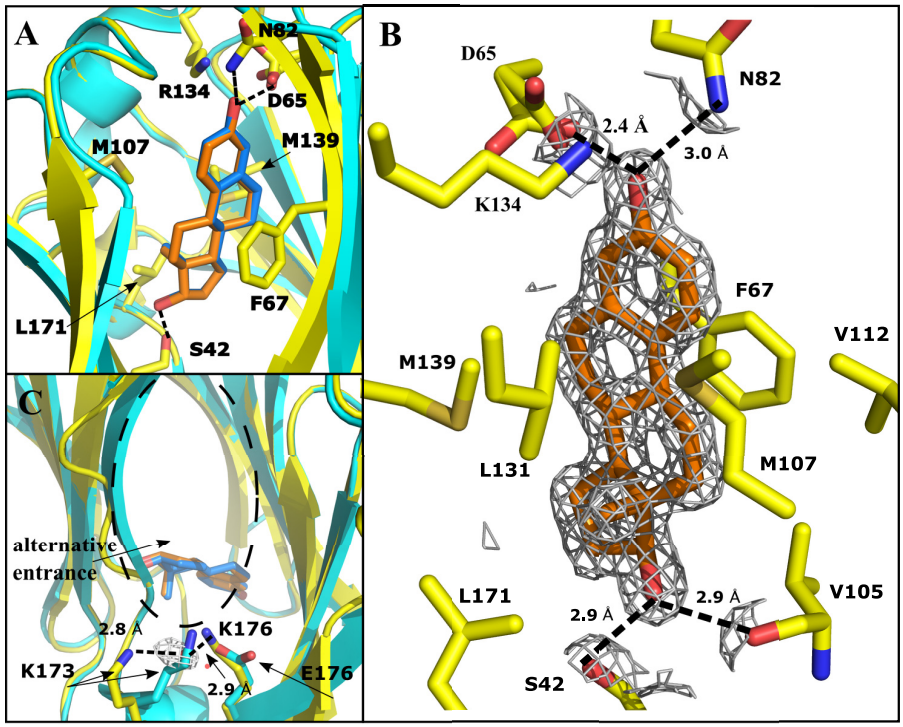

Figure 2. Crystal structure of estradiol (*orange*) bound to the LG4 domain of E176K SHBG (*yellow*) modeled at 1.73 Å resolution. Hydrogen bonds are indicated as *dotted lines*. Structure of WT SHBG-bound estradiol (PDB: 1LHU) (*cyan*, with estradiol highlighted *blue*) is overlaid for comparison. *A*, overlay of E176K SHBG and WT SHBG with estradiol bound, highlighting the similarity of the two structures and steroid positioning. One cycle alignment RMSD = 1.25 Å across all Cα atoms. All key residue side chains are in the same position for both structures. *B*, estradiol positioned in the binding pocket of E176K SHBG with residues involved in the binding interaction shown. $2F_o - F_c$ map is shown around the ligand at 1.5 σ, carved at 3.0 Å. *C*, proposed alternative entrance to the binding pocket is shown, with the E176K substitution and resulting hydrogen bond interaction with Lys-173 through a water molecule (*red*) shown.

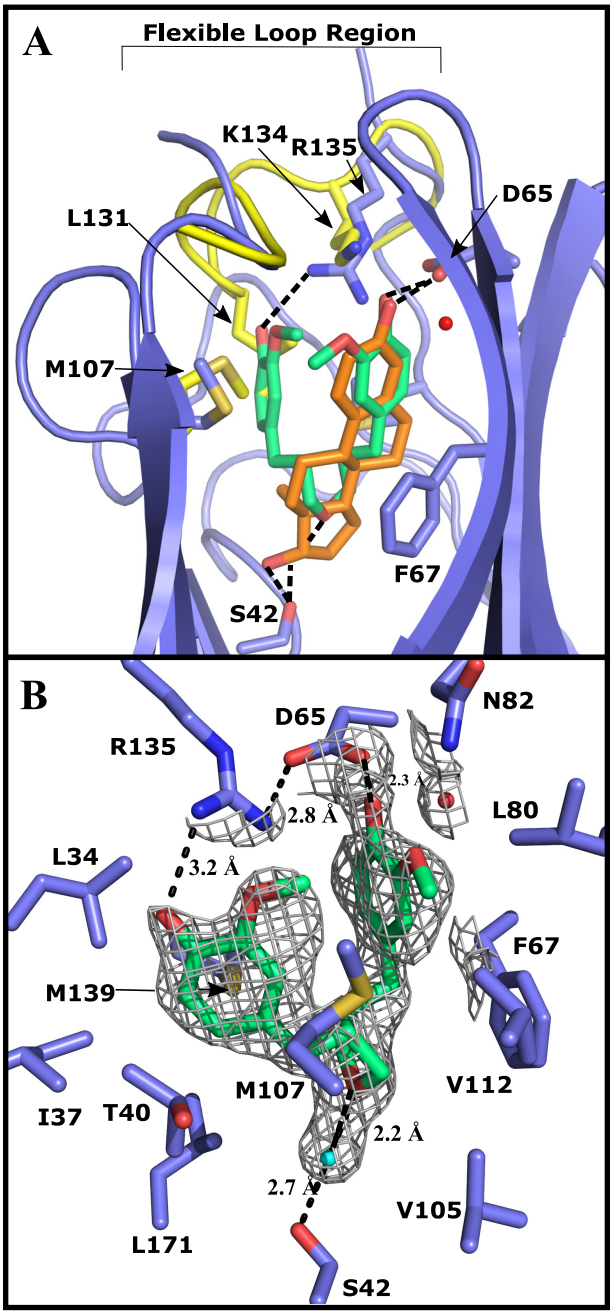

Figure 3. Crystal structure of DVT (*green*) bound to the LG4 domain of E176K SHBG (*blue*) modeled at 1.80 Å resolution. An overlay of the differences between the crystal structure of E176K estradiol (*yellow*, estradiol is *orange*) and the DVT-bound E176K SHBG highlights the key differences around the binding pocket. One cycle alignment RMSD = 1.02 Å across all Cα atoms. Water molecules involved in the binding are shown as *red spheres* and hydrogen bonds are indicated as *dotted lines*. *A*, DVT-SHBG (*blue*) is aligned with estradiol-SHBG (*yellow*) with the differences in the flexible loop region (disordered in DVT structure) and key residues indicated. DVT and estradiol are compared in the binding site highlighting the differences in the volume occupied by the nonsteroidal ligand. *B*, DVT binding interactions and the residues forming the hydrophobic pocket are shown. $2F_o - F_c$ electron density at 1.0 σ and carved at 3.0 Å is shown around DVT and the water molecules in the binding pocket.

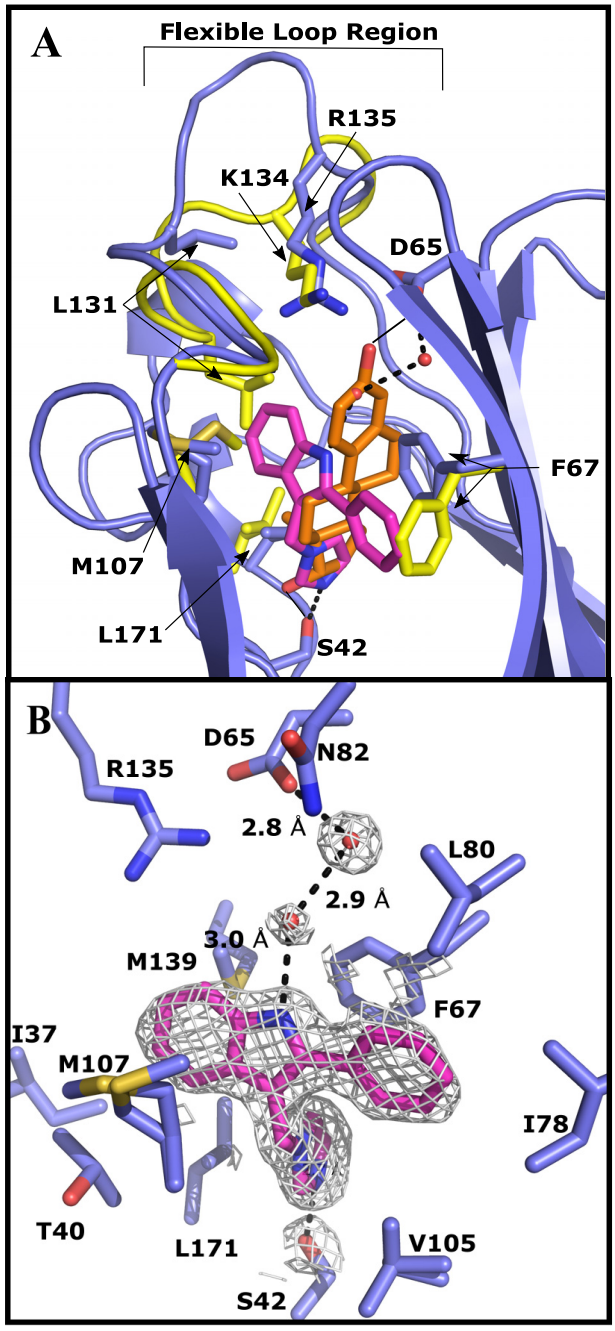

Figure 4. Crystal structure of IPI (*purple*) bound to the LG4 domain of E176K SHBG (*blue*) modeled at 1.71 Å resolution. An overlay of the differences between the crystal structure of E176K estradiol (*yellow*, estradiol is *orange*) and the IPI-bound E176K SHBG highlights the key differences around the binding pocket. One cycle alignment RMSD = 1.35 Å across all Cα atoms. Water molecules involved in the binding are shown as *red spheres* and hydrogen bonds are indicated as *dotted lines*. *A*, IPI-SHBG (*blue*) is aligned with estradiol-SHBG (*yellow*) with the differences in the flexible loop region and key positions of key residues indicated. IPI and estradiol are compared in the binding site highlighting the differences in the volume occupied by the nonsteroidal ligand. *B*, IPI binding interactions and the residues forming the hydrophobic pocket are shown. $2F_o - F_c$ electron density (1.5 σ) is shown around DVT and the water molecules in the binding pocket.

structure, and this space is filled by water molecules (Fig. 4*B*). Although Asp-65 is 6.9 Å away from IPI, two of these water molecules imply binding through a water molecule bridge ending at the nitrogen of the IPI indole group (Fig. 4*B*). The coordination of these water molecules appears to be supported by Arg-135, Asn-82, and Ser-128. Other residues that are important in accommodating steroids are integral to the hydrophobic pocket, and include Met-107 and Met-139 (3). In the IPI structure, Met-107 is modeled with multiple conformations appearing to increase the hydrophobic area to accommodate the

Table 2

IPI and DVT competitive binding analysis of CHO expressed SHBG mutants of key binding interaction residues identified from the structure model

For WT SHBG and different SHBG mutants, IC_{50} values for IPI and DVT were calculated from competitive displacement of [^{3}H]DHT using unlabeled DHT as the reference. Errors were established using the 95% confidence interval of the IC_{50} values produced from nine concentration point displacement curves. The RBA values were calculated by expressing the DHT IC_{50} values of IPI or DVT as a percentage of the DHT IC_{50}s for WT SHBG or given mutant, thereby allowing comparisons of mutants where DHT affinity was also changed relative to WT SHBG. NCD, no competitive displacement.

SHBG mutant	DHT IC_{50} (nM)	IPI IC_{50} (nM)	DVT IC_{50} (nM)	IPI (RBA%)	DVT (RBA%)
Wildtype	4.7 ± 0.7	55 ± 7	2500 ± 370	8.5	0.19
D65A	4.0 ± 1.8	430 ± 160	NCD	0.93	NCD
M107V	3.6 ± 1.0	7.6 ± 1.3	690 ± 350	47	0.52
M139V	4.6 ± 1.7	41 ± 27	590 ± 370	11	0.78
F67A	5.1 ± 1.6	390 ± 240	820 ± 320	1.3	0.62
R135L	3.0 ± 0.6	30 ± 13	3100 ± 1600	10	0.10
N82A	3.3 ± 1.2	23 ± 7	310 ± 180	14	1.1
E176K	14 ± 2	150 ± 16	4200 ± 790	9.3	0.33
S42A	42 ± 9	NCD	4100 ± 950	NCD	1.0

indole portion of IPI (Fig. 4*B*). Additionally, Leu-171 projects 1.0 Å further into the binding pocket when compared with when estradiol is present (Fig. 4*A*). As in the DVT-bound structure, IPI binding shifts the loop region above the steroid-binding site outwards, as a result of Leu-131 being displaced by the indole of IPI, and this also causes Lys-134 to move out of the binding pocket and Arg-135 to orient toward the binding pocket. In the IPI-bound structure, Trp-84 is positioned as it is when DHT is bound (PDB: 1D2S).

Validation of SHBG interactions with the nonsteroidal ligands DVT and IPI

Substitutions of specific residues within the N-terminal LG domain of SHBG were made to validate crystal structure predictions of the interactions between SHBG and DVT or IPI (Table 2). Surprisingly, a S42A substitution that reduces affinity for DHT (19) resulted in an ~5-fold increased relative binding affinity (RBA) for DVT when compared with that of DHT (Table 2). By contrast, a D65A substitution abolished DVT binding to SHBG, supporting the assumption that Asp-65 hydrogen bonds with the hydroxyl of vanillyl A. The binding of DVT was also negatively impacted by the substitution of Arg-135 with leucine. The N82A substitution resulted in an increase in the RBA of DVT, likely caused by a more optimal conformation of the methoxy of vanillyl group A, as it appears that Asn-82 does not contribute a significant hydrogen bond to this interaction. Substitutions of residues within the hydrophobic pocket, Met-107, Met-139, and Phe-67 by smaller amino acids, resulted in modestly increased RBA for DVT (Table 2).

The most significant residues contributing to IPI binding from the crystal structure appear to be Asp-65, Ser-42, and Phe-67. A D65A substitution decreases the RBA of IPI (Table 2) that is unlikely to be because of a structural change in the binding site, but it supports the possibility that Asp-65 contributes a hydrogen bond through water molecules (Fig. 3*A*). The SHBG S42A mutant showed no detectable competitive binding for IPI, supporting the predicted hydrogen bond between IPI and Ser-42. Study of the SHBG R135L mutant indicates that this residue does not contribute significantly to the binding of IPI, as was also observed for the N82A substitution. However, substitution

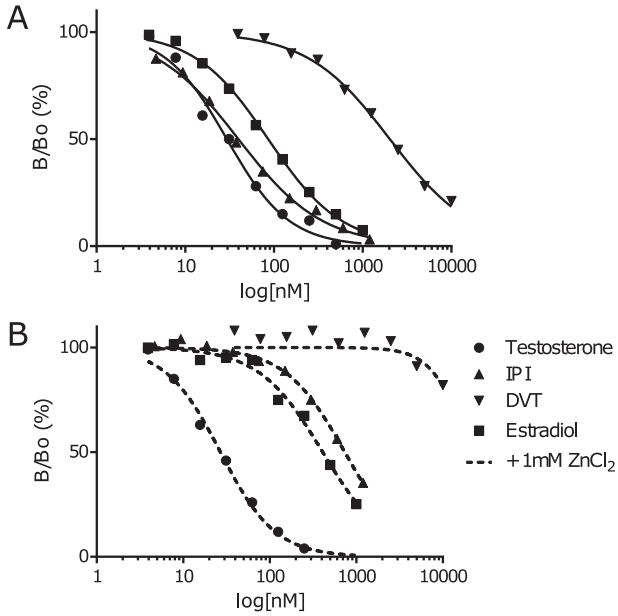

Figure 5. Competitive steroid binding assays. *A*, steroid binding assays preformed on diluted human serum, using [3H] DHT as a tracer, and unlabeled IPI, DVT, estradiol, and testosterone at increasing concentrations to establish displacement curves. The relative binding affinity of IPI, DVT, and estradiol compared with testosterone we found to be 74, 1.5, and 34%, respectively. *B*, competitive steroid-binding assays assess IPI, DVT, estradiol, and testosterone at increasing concentrations to establish displacement curves with the addition of 1 mM zinc chloride. The relative binding affinity of IPI, DVT, and estradiol compared with testosterone in the presence of zinc was found to be 3.7%, no binding, and 6.6%, respectively.

of hydrophobic residues in the steroid-binding pocket caused changes in the affinity of SHBG for IPI. The F67A substitution greatly reduced the RBA of SHBG for IPI, which was expected because of the predicted importance to binding of the π-π stacking interaction occurring between the phenyl groups of IPI and Phe-67. The SHBG M139V mutant did not change the RBA for IPI, whereas the M107V mutant appears to have an increased affinity for IPI. Given the multiple conformations of Met-107 in the IPI-bound SHBG structure, it is reasonable to assume that the substitution of this residue with a smaller hydrophobic residue likely allows the orientation of IPI to be adjusted allowing for other interactions to be optimized.

Influence of high Zn^{2+} concentrations on the binding of DVT and IPI to SHBG

The relative affinities of SHBG for DVT and IPI were 1.5 and 74% of that measured for testosterone, respectively (Fig. 5*A*). These competition curves also demonstrate that the affinity for DVT is considerably lower than that of estradiol (34.2%), whereas IPI binds with a higher affinity than estradiol and almost as well as testosterone (Fig. 4*A*). We also found that (−)3,4-dibenzyltetrahydrofuran, a compound lacking the hydroxyl and methoxy groups of DVT, binds SHBG very poorly with an IC_{50} value >10 μM.

Saturation of the SHBG zinc-binding site within the flexible loop region that covers the steroid binding pocket was also tested to determine how this might influence the relative binding affinities for DVT and IPI (Fig. 5*B*). This demonstrated that the affinities of SHBG for DVT and IPI were both negatively impacted in the presence of high Zn^{2+} concentrations. Under

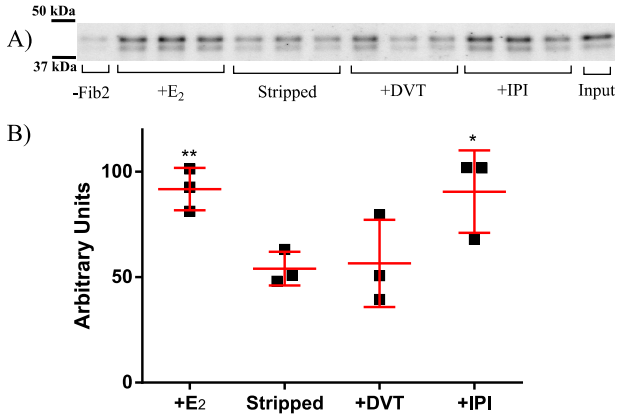

Figure 6. Ligand-dependent interaction between SHBG and fibulin-2. *A*, GST:fibulin-2 (1081–1157) was immobilized on GSH beads and incubated overnight with diluted serum containing 20 nM human SHBG, in the presence and absence of 100 nM estradiol, DVT, or IPI. The beads were washed and then boiled in SDS loading buffer for analysis by Western blotting. *B*, this graph shows the relative amount of SHBG immunoreactivity (mean ± S.D. in *red* with individual data points as *black squares*) for each condition as measured by densitometry of three pulldowns shown in the above Western blotting. Significant differences determined using an unpaired *t* test from the stripped control, to which no ligand was added, are as indicated; *, $p < 0.05$; **, $p < 0.005$.

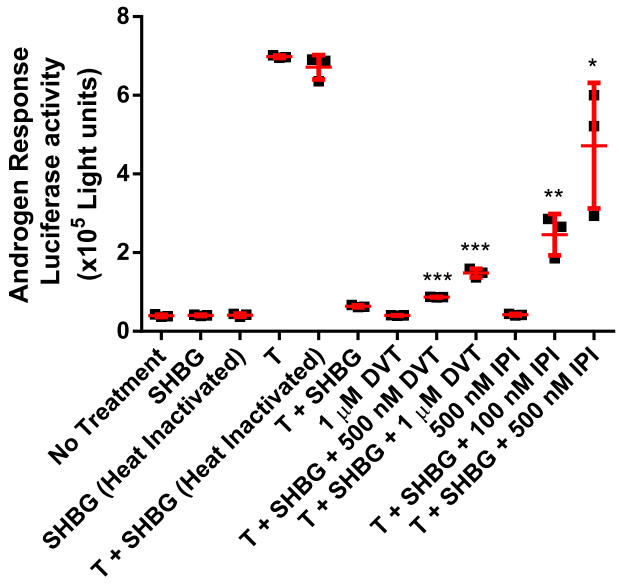

Figure 7. CV1 SHBG-dependent androgen response assay luciferase data indicating that SHBG restricts the bioavailability of testosterone and nonsteroidal ligands are capable of increasing the bioavailability in a dose-dependent manner. DVT was found to slightly increase the bioavailability of testosterone (*T*), whereas IPI was significantly more effective. Data are from three experiments expressed as mean ± S.D. in *red* with individual data points as *black squares*. An unpaired *t* test was applied to compare the statistically significant difference between experimental samples to the T + SHBG baseline. *, $p < 0.05$; **, $p < 0.005$;***, $p < 0.0005$. Heat treatment of SHBG confirmed that no androgens remained bound to SHBG after stripping and purification.

these conditions, the SHBG affinity for testosterone is unchanged whereas its affinity for estradiol is markedly reduced (Fig. 5, *A versus B*), as reported previously (11). In the presence of high Zn^{2+} concentrations, DVT showed no detectable binding at all, whereas the affinity of SHBG for IPI was markedly reduced (by ~20-fold) when compared with that of testosterone (Fig. 5*B*), and this effect was greater than ~5-fold reduction in the affinity for estradiol, relative to that of testosterone.

Interaction between SHBG and fibulin-2 is influenced DVT and IPI

The influence of DVT and IPI on the ligand-dependent interaction between SHBG and fibulin-2 was assessed in a GST:fibulin-2 pulldown assay followed by Western blotting. A negative control (Sepharose linked to GST alone) confirmed that the presence of the carboxyl-terminal region of fibulin-2 is required to pull down human SHBG from a diluted serum sample (Fig. 6*A*). As reported previously (20), the saturation of the SHBG-binding site by estradiol under these conditions increased the interaction between fibulin-2 and SHBG significantly ($p = 0.007$), when compared with that observed using unliganded SHBG (Fig. 6*B*). Importantly, this interaction was not influenced by the binding of DVT to SHBG, whereas IPI enhanced the SHBG interaction with fibulin-2 significantly ($p = 0.0403$), and to a similar extent as that observed when the SHBG-binding site was fully occupied by estradiol (Fig. 6*B*).

DVT and IPI enhance the bioavailability of testosterone

Using a cell line that stably expresses the androgen receptor and a luciferase reporter gene under the control of an androgen response element, we measured how the competitive displacement of testosterone from SHBG in culture media by DVT or IPI influenced androgen responses. The results indicate that the addition of 10 nM SHBG alone to the culture medium has no effect in the absence of testosterone, nor did the same concentration of heat-inactivated SHBG (Fig. 7). In the absence of SHBG, a robust ~15-fold increase in luciferase response was observed upon treatment with 10 nM testosterone, and the presence of heat-inactivated SHBG had no effect on this. By contrast, the presence of 10 nM SHBG almost completely suppressed the activity of the same concentration of testosterone. The addition of 1 μM DVT alone did not cause an androgen response, whereas the addition of 500 nM ($p = 0.0001$) and 1 μM DVT ($p = 0.0002$) both cause significant increases in androgen activity when incubated together with 10 nM SHBG and 10 nM testosterone. The addition of 500 nM IPI alone also had no effect on androgen response and was much more effective in increasing androgen responses in the presence of 10 nM SHBG and 10 nM testosterone at both the 100 nM ($p = 0.004$) and 500 nM ($p = 0.0114$) concentrations, as compared with DVT. This likely reflects the much higher affinity of SHBG for IPI when compared with DVT (Fig. 5*A*).

Discussion

The N-terminal laminin G domain of the natural SHBG mutant E176K crystalizes efficiently and represents an ideal structure for crystallization studies. Although it has an increased affinity for estradiol (13), it binds DVT or IPI with affinities similar to those of WT SHBG (Table 2). Our crystal structure data suggest that the higher affinity of SHBG E176K for estradiol may be because of an increase in the size of an alternative entrance to the binding pocket (13), as illustrated (Fig. 2). The increased affinity of SHBG E176K for estradiol is explained by the outward displacement of Lys-173 at the rim of

this possible entrance to the steroid-binding pocket. Importantly, because the affinities of IPI and DVT for SHBG E176K *versus* WT SHBG are virtually identical, these nonsteroidal ligands probably do not access the steroid-binding site in the same manner as estrogens.

The crystal structures of SHBG-bound DVT or IPI provide insight into how the steroid-binding pocket accommodates ligands that do not resemble the typical cyclopentanophenanthrene structure of steroids. The large volume occupied by DVT in the steroid-binding site and the presence of a water molecule bridging the ligand–Ser-42 hydrogen bond is unique to the DVT-bound SHBG structure. Moreover, this water-bridged hydrogen bond does not appear to be as important an interaction for binding as it is for steroid ligands or IPI, as demonstrated by the increased affinity of the SHBG S42A mutant for DVT. Indeed, we predict that the increased affinity of SHBG S42A for DVT is caused by the removal of the water molecule bridging the hydrogen bond interaction, allowing for DVT to be positioned deeper into the binding pocket, thereby optimizing other interactions with the function groups of DVT.

The contrasting positioning of Arg-135 and Lys-134 in the DVT-bound *versus* steroid-bound SHBG structures shows that the flexible loop region over the steroid-binding pocket is adaptable, and can fulfill its role of stabilizing ligand binding through direct interactions with both the ligand and the surrounding residues. The apparent interaction between Arg-135 and Asp-65 in the DVT-bound SHBG structure may replace the coordination of Asp-65 by Thr-60 seen when steroids are bound (10). The role of Arg-135 also follows closely the stabilizing role of Lys-134 when SHBG is bound by steroids (9). The binding of DVT requires an interaction with Asp-65 that anchors the molecule near the entrance to the binding pocket, contrasting with steroids that only show a reduction in affinity when Asp-65 is unable to hydrogen bond. The observations made from the study of DVT show how SHBG binds small nonsteroidal compounds with even modest affinity. Moreover, the unique position of DVT within the SHBG ligand-binding site provides a framework for modeling studies (14, 21–23) to identify other molecules that bind SHBG with greater affinity.

The crystal structure of IPI bound to SHBG also demonstrates a conformation of the binding pocket that has not been described previously. This unique conformation allows for key residues involved in binding steroids to maintain their role, while changing the topography of the hydrophobic pocket. For example, the alternate conformation of Phe-67 accommodates the unique orientation of IPI relative to steroids (Fig. 4*A*). The presence of four water molecules in the binding site of the IPI-bound SHBG crystal structure is also novel for SHBG ligands. The key hydrogen bond interaction between IPI and Asp-65 is coordinated through two organized water molecules, incurring an entropic cost of the binding. Similarly, the altered Phe-67 conformation may contribute negatively to the overall binding energy of IPI. Interestingly, these energetic penalties are overcome by the positioning of IPI in the binding pocket and the strength of the ligand-protein interactions allowing IPI to be bound with high affinity. Modifications to the IPI structure that maintain Asp-65 hydrogen bonding without the need of organized water molecules could result in a higher affinity for SHBG. Moreover, the flexibility of the SHBG binding pocket to accommodate IPI, like DVT, suggests that SHBG is capable of binding a wider range of nonsteroidal molecules, in this novel binding pocket orientation, with higher affinities than reported to date.

The binding of DVT and IPI by SHBG is altered by the presence of zinc, as is the case for estradiol (11). When zinc is present, Asp-65 is in an alternate conformation limiting its ability to interact with ligands, and this causes a similar removal of the hydrogen bonding partner, as expected in the SHBG D65A mutant that has a reduced affinity for IPI and no measurable DVT binding. The significance of the affinity changes for estrogens caused by zinc is unclear, but it may influence the role of SHBG in specific anatomical locations where zinc concentrations are very high, such as in the male reproductive tract (11). This similarity in the way SHBG loses affinity for these nonsteroidal ligands and estrogens in the presence of high concentrations of zinc raises the question of whether they modify other activities of SHBG in ways that are enhanced most effectively by estrogens, such as interactions with members of the fibulin family of matrix-associated proteins (20).

Human SHBG interacts with the carboxyl-terminal domains of the matrix associated proteins, fibulin-2 and fibulin-1D, in a steroid-ligand– dependent manner (20). This interaction occurs most efficiently when the steroid-binding site was occupied by estradiol, and occupancy of the SHBG steroid-binding site by estradiol appears to promote the extravascular sequestration of plasma SHBG in some tissues (20). We therefore examined whether DVT or IPI interactions with SHBG might alter its interactions with fibulin-2. Unlike estradiol, the binding of DVT to SHBG did not increase its interaction with fibulin-2, whereas IPI promoted a similar interaction between SHBG and fibulin-2 as that observed when its binding site is occupied by estradiol. The fibulin-2 binding of SHBG that is enhanced by estradiol has been attributed to a structural difference in SHBG when androgens and estrogens are bound, primarily around the flexible loop region of its amino-terminal LG domain (14, 20). The structure of IPI does not clarify this because the loop region is organized in the IPI-bound SHBG and differs in orientation as compared to when estradiol is bound. Moreover, the position of Trp-84 varies between the IPI-bound and estradiol-bound structures which both bind fibulin. Although the exact interactions behind the binding of SHBG to fibulin-2 have yet to be deciphered, the enhancement of this interaction by IPI, in contrast with the lack of effect of androgens or DVT, suggest that the binding of IPI to SHBG may promote its compartmentalization in specific tissues in the body in a manner similar to observed for estradiol-bound SHBG (20).

The primary roles of SHBG are to transport sex steroids in plasma and extravascular compartments and to control the amounts of sex steroids that can access target cells (2). Additionally, it represents a reservoir of sex steroids that is protected from metabolic clearance. This reservoir also offers an opportunity to liberate endogenous steroids from their SHBG-binding site by displacement with a competitive ligand. To test this, CV1 cells that express the androgen receptor and a luciferase reporter under the control of an androgen response element

were used to determine whether testosterone could be displaced from SHBG by nonsteroidal ligands *in vitro*. Our results show that both IPI and DVT are effective in this manner and enhance androgen action in this reporter system. Moreover, the luciferase responses are directly related to the relative affinities of SHBG for DVT and IPI. These results are interesting because DVT is reported to be the active component of natural health products that are claimed to increase the bioavailability of testosterone (18). There is therefore reason to believe that high affinity nonsteroidal ligands of SHBG like IPI may offer a much more effective way to liberate steroids from SHBG in biological fluids, thereby augmenting the activities of endogenous steroids or exogenous steroids used for hormone replacement. In this context, it is important to note that the affinity of SHBG for IPI not only approaches that of testosterone but is several times greater than that of estradiol. Thus, in addition to increasing androgen action as shown in our *in vitro* experiments, compounds such as IPI could be used to enhance both androgen and estrogen action through their competitive displacement from SHBG *in vivo*. The crystal structures we have obtained for SHBG in complex with these nonsteroidal compounds, and the ways they act to alter SHBG activities in different contexts, also provide a framework for additional design of even more potent ligands that could be used for these purposes.

Experimental procedures

SHBG ligands

Steroids, DHT, testosterone, and estradiol (Steraloids) and [^{3}H]DHT (specific activity 60 Ci/mmol, PerkinElemer Life Sciences) were used without further purification. DVT and a DVT-related compound, 3,4-dibenzyltetrahydrofuran, were synthesized in purities of >98% (24). A preparation of IPI was kindly provided by Pfizer and used for the purification of the human SHBG N-terminal LG domain in *Escherichia coli* and obtained commercially (Enamine) at >95% purity for crystallographic determinations and biochemical analyses.

Human SHBG for crystallography

The N-terminal LG domain (residues 1–205 of the mature polypeptide) of SHBG E176K was expressed as a GSH-S transferase (GST) fusion protein in a pGEXT2 expression vector (GE Healthcare) in Rosseta™ *E. coli* (MilliporeSigma). Cultures were grown to 0.7 A_{600} before induction with 0.2 mM isopropyl 1-thio-β-D-galactopyranoside at 22 °C for 16 h. Cells were collected and lysed by sonication in Tris-buffered saline (50 mM Tris, 150 nM NaCl, pH 8.5) + 2.5 mM $CaCl_2$ + 5 μM estradiol, DVT or IPI. Cell lysates were spun at 30,000 × *g* for 30 min and then passed across a 10-ml bed of Pierce GSH Superflow Agarose beads (Thermo Fisher Scientific) at room temperature. The column was then washed with 10 volumes of the same buffer before on-column cleavage with a column volume of 10 units of thrombin/milliliter overnight at room temperature. After elution, fractions containing SHBG steroid-binding activity were pooled and concentrated for FPLC purification using a Superdex® 75 size exclusion chromatography column (GE Healthcare). Size exclusion fractions containing SHBG were pooled and mixed with Pierce™ Glutathione Magnetic Agarose Beads for 4 h at room temperature to remove any residual GST before concentration in an Amicon® Ultra 3000 MWC centrifugal filter (MilliporeSigma) to 10 mg/ml, and then buffer exchanged to 50 mM HEPES, pH 7.5, containing 2.5 mM $CaCl_2$ and 10 μM estradiol, DVT, or IPI.

Crystallization and structure determination

Crystals of SHBG E176K were grown using the hanging drop method in a reservoir solution of 20% PEG 3350, 0.2 M potassium thiocyanate, and 5 μM estradiol or 10 μM DVT or IPI at 22 °C. Crystals of SHBG E176K in complex with estradiol were grown using 1 μl of protein solution mixed with 1 μl of reservoir solution. Crystals appeared within 48 h and grew to maximum size after 5 days. In light of the ease of crystallization, the reliability of diffraction data collection, and similarity between the estradiol-bound SHBG E176K crystal structures and other available crystals structures of SHBG, we used SHBG E176K for further crystallization studies.

Crystals of SHBG in complex with DVT or IPI were grown in the same way, with an additional seeding of a 1:10,000 dilution of a crushed estradiol-bound SHBG E176K crystal to facilitate crystallization and growth to a maximal size in 5 days. Crystals were frozen in a cryo-solution of 30% ethanol, 20% PEG 3350, 0.2 M potassium thiocyanate, and 14 μM estradiol or 10 μM IPI or DVT for data collection. Diffraction data for SHBG in complex with estradiol were collected at the Stanford Synchrotron Radiation Lightsource (SSRL, Stanford, CA) and processed using HKL3000 (25). Diffraction data for DVT and IPI were collected at the Advanced Photon Source beamline and processed using XDS (26). All phases were determined by molecular replacement with Phaser (27) using a previously solved SHBG complexed estradiol structure (PDB 1LHU) as the search model for SHBG E176K in complex with estradiol, which was then used as the search model for both DVT- and IPI-bound SHBG structures. Models were completed with iterative cycles of manual model building in Coot (28) and refinement with PHENIX (29). Prior to the addition of ligand structures to the model, electron density was assessed to ensure ligand density was present and complete (Fig. S1). RSRZ outliers occurred in all structures in the amino and carboxyl termini, as well as the flexible loop near the binding pocket; this is consistent with previously published structures of SHBG. Structure files are available from the RCSB database with accession codes 6PYF, 6PYB, and 6PYA, for estradiol-bound, DVT-bound, and IPI-bound E176K SHBG structures, respectively.

Human SHBG and mutants with amino acid substitutions

Serum from transgenic mice containing high concentrations of human SHBG (30) was treated twice at 37 °C for 30 min with dextran-coated charcoal (DCC) to remove steroids and then diluted 10-fold in 20 mM Tris, pH 7.5, prior to FPLC Mono-Q™ column chromatography (GE Healthcare) to separate SHBG from albumin. Fractions containing SHBG, as confirmed by steroid-binding activity, were pooled and treated with DCC twice at 37 °C for 30 min to remove steroids. The sample was then concentrated, and buffer exchanged using a 10-kDa molecular weight cut-off Amicon® centrifugal filter into phenol red free DMEM-F12 medium (Thermo Fisher Scientific) con-

taining 10% charcoal stripped fetal bovine serum (FBS) for use in androgen response assays (31).

To produce human SHBG mutants with specific amino acid substitutions, an SHBG cDNA in PRC/CMV was used to create expression vectors for the desired mutant SHBG, as described previously (13). Plasmids were transfected into CHO-S cells using Lipofectamine 2000 (Invitrogen), and cells were grown under 1 mg/ml G418 selection in MEM α containing antibiotics (penicillin and streptomycin) and 10% FBS for 3 weeks to generate stable cell lines. Stable cell lines were grown to ~80% confluence before the media were changed to HyClone™ SFM4 CHO-utility™ (Fisher Scientific) plus antibiotics and 100 nM DHT for 5 days before media containing SHBG were harvested for analysis.

Steroid-binding assays

A steroid ligand saturation analysis was used to measure the steroid-binding capacity of SHBG and its RBA for different ligands (32). Briefly, CHO media or a human serum sample containing 94 nM SHBG were treated with DCC to remove steroids prior to equilibration with [^{3}H]DHT in the presence or absence of 100-fold molar excess DHT to determine nonspecific binding. Unbound steroid was removed by exposure to DCC for 10 min at 0 °C followed by centrifugation, allowing for the SHBG-bound [^{3}H]DHT to be measured. The RBA values were determined by using [^{3}H]DHT as the labeled ligand and increasing amounts of competitors in the presence or absence of 1 mM $ZnCl_2$ (11, 32).

Fibulin-2 pulldown assay

A GST:fibulin-2 fusion protein was produced in BL21 *E. coli* using cDNA encoding carboxyl-terminal residues 1081–1157 of fibulin-2 in pGEX KGK (Amersham Bioscience), as described previously (20). Briefly, bacterial cultures were grown to 0.7 A_{600} before induction with 0.2 mM isopropyl 1-thio-β-D-galactopyranoside at 22 °C for 16 h. Cells were collected and lysed by sonication in Tris-buffered saline + 0.02% Triton X-100. Cell lysates were spun at 30,000 × *g* for 30 min and then processed by batch over 1 ml of Pierce GSH Superflow Agarose beads (Thermo Fisher Scientific) at 4 °C. The beads were then washed with 10 volumes of the same buffer before use in pulldown assays. A GST empty vector, pGEX KGK, was expressed and purified following the same protocol as a negative control. Transgenic mouse serum containing 20 nM human SHBG was treated twice with DCC at 37 °C before 100 nM estradiol, DVT, or IPI was added. Overnight incubation with SHBG and 50 μl of GST:fibulin-2 beads or GST beads was performed at 4 °C in binding buffer (20 mM Tris-HCl, pH. 8.0, 0.02% Nonidet P-40). Beads were sedimented and washed three times with ice-cold binding buffer before being boiled in SDS-PAGE loading buffer for 5 min for the detection of SHBG by Western blotting (20).

Androgen response assay

Monkey CV1 cells stably transfected with androgen receptor and an androgen receptor response element *Gaussia* luciferase construct (31) were kindly provided by Dr. William Rainey (Ann Arbor, MI). The CV1 cells were seeded in 48-well plates at 40,000 cells/well and cultured in phenol red free DMEM-F12 supplemented with 10% charcoal-stripped (steroid free) FBS and antibiotics. The following day the cells were treated with 10 nM SHBG and 10 nM testosterone in the absence or presence of increasing amounts of DVT or IPI, and 10 nM heat-inactivated (1 h at 60 °C) SHBG was used as a negative control. After 16 h, the culture medium was collected for luciferase analysis on a Victor^{3}V plate reader (PerkinElmer), as described (31).

Author contributions—P. R., F. V. P., and G. L. H. conceptualization; P. R. data curation; P. R. formal analysis; P. R., S. D., and T.-S. W. investigation; P. R., S. D., and F. V. P. methodology; P. R. writing-original draft; K. W. resources; F. V. P. validation; F. V. P. and G. L. H. project administration; G. L. H. supervision; G. L. H. funding acquisition; G. L. H. writing-review and editing.

Acknowledgment—We thank Caroline Underhill for technical support throughout this project.

References

1. Mendel, C. M. (1989) The free hormone hypothesis: A physiologically based mathematical model. *Endocr. Rev.* **10,** 232–274 CrossRef Medline
2. Hammond, G. L. (2016) Plasma steroid-binding proteins: Primary gatekeepers of steroid hormone action. *J. Endocrinol.* **230,** R13–R25 CrossRef Medline
3. Grishkovskaya, I., Avvakumov, G. V., Sklenar, G., Dales, D., Hammond, G. L., and Muller, Y. A. (2000) Crystal structure of human sex hormone-binding globulin: Steroid transport by a laminin G-like domain. *EMBO J.* **19,** 504–512 CrossRef Medline
4. Avvakumov, G. V., Grishkovskaya, I., Muller, Y. A., and Hammond, G. L. (2001) Resolution of the human sex hormone-binding globulin dimer interface and evidence for two steroid-binding sites per homodimer. *J. Biol. Chem.* **276,** 34453–34457 CrossRef Medline
5. Bocchinfuso, W. P., and Hammond, G. L. (1994) Steroid-binding and dimerization domains of human sex hormone-binding globulin partially overlap: Steroids and Ca2+ stabilize dimer formation. *Biochemistry* **33,** 10622–10629 CrossRef Medline
6. Cousin, P., Déchaud, H., Grenot, C., Lejeune, H., and Pugeat, M. (1998) Human variant sex hormone-binding globulin (SHBG) with an additional carbohydrate chain has a reduced clearance rate in rabbit. *J. Clin. Endocrinol. Metab.* **83,** 235–240 CrossRef Medline
7. Cousin, P., Déchaud, H., Grenot, C., Lejeune, H., Hammond, G. L., and Pugeat, M. (1999) Influence of glycosylation on the clearance of recombinant human sex hormone-binding globulin from rabbit blood. *J. Steroid Biochem. Mol. Biol.* **70,** 115–121 CrossRef Medline
8. Dunn, J. F., Nisula, B. C., and Rodbard, D. (1981) Transport of steroid hormones: Binding of 21 endogenous steroids to both testosterone-binding globulin and corticosteroid-binding globulin in human plasma. *J. Clin. Endocrinol. Metab.* **53,** 58–68 CrossRef Medline
9. Grishkovskaya, I., Avvakumov, G. V., Hammond, G. L., Catalano, M. G., and Muller, Y. A. (2002) Steroid ligands bind human sex hormone-binding globulin in specific orientations and produce distinct changes in protein conformation. *J. Biol. Chem.* **277,** 32086–32093 CrossRef Medline
10. Avvakumov, G. V., Grishkovskaya, I., Muller, Y. A., and Hammond, G. L. (2002) Crystal structure of human sex hormone-binding globulin in complex with 2-methoxyestradiol reveals the molecular basis for high affinity interactions with C-2 derivatives of estradiol. *J. Biol. Chem.* **277,** 45219–45225 CrossRef Medline
11. Avvakumov, G. V., Muller, Y. A., and Hammond, G. L. (2000) Steroid-binding specificity of human sex hormone-binding globulin is influenced by occupancy of a zinc-binding site. *J. Biol. Chem.* **275,** 25920–25925 CrossRef Medline
12. Grishkovskaya, I., Avvakumov, G. V., Hammond, G. L., and Muller, Y. A. (2002) Resolution of a disordered region at the entrance of the human sex hormone-binding globulin steroid-binding site. *J. Mol. Biol.* **318,** 621–626 CrossRef Medline

13. Wu, T. S., and Hammond, G. L. (2014) Naturally occurring mutants inform SHBG structure and function. *Mol. Endocrinol.* **28,** 1026–1038 CrossRef Medline
14. Avvakumov, G. V., Cherkasov, A., Muller, Y. A., and Hammond, G. L. (2010) Structural analyses of sex hormone-binding globulin reveal novel ligands and function. *Mol. Cell Endocrinol.* **316,** 13–23 CrossRef Medline
15. Hodgert Jury, H., Zacharewski, T. R., and Hammond, G. L. (2000) Interactions between human plasma sex hormone-binding globulin and xenobiotic ligands. *J. Steroid Biochem. Mol. Biol.* **75,** 167–176 CrossRef Medline
16. Schöttner, M., Gansser, D., and Spiteller, G. (1997) Lignans from the roots of *Urtica dioica* and their metabolites bind to human sex hormone binding globulin (SHBG). *Planta Med.* **63,** 529–532 CrossRef Medline
17. Schöttner, M., Spiteller, G., and Gansser, D. (1998) Lignans interfering with 5α-dihydrotestosterone binding to human sex hormone-binding globulin. *J. Nat. Prod.* **61,** 119–121 CrossRef Medline
18. McDonald, T. J., Perry, M. H., Jones, A. G., Donohoe, M., Salzmann, M. B., and O'Connor, J. (2011) A novel case of a raised testosterone and LH in a young man. *Clin. Chim. Acta.* **412,** 1999–2001 CrossRef Medline
19. Hong, E.-J., Sahu, B., Jänne, O. A., and Hammond, G. L. (2011) Cytoplasmic accumulation of incompletely glycosylated SHBG enhances androgen action in proximal tubule epithelial cells. *Mol. Endocrinol.* **25,** 269–281 CrossRef Medline
20. Ng, K.-M., Catalano, M. G., Pinós, T., Selva, D. M., Avvakumov, G. V., Munell, F., and Hammond, G. L. (2006) Evidence that fibulin family members contribute to the steroid-dependent extravascular sequestration of sex hormone-binding globulin. *J. Biol. Chem.* **281,** 15853–15861 CrossRef Medline
21. Hazarika, J., Ganguly, M., and Mahanta, R. (2019) Molecular interactions of chlorpyrifos and its environmental degradation products with human sex hormone-binding globulin: An in silico study. *J. Appl. Toxicol.* **39,** 1002–1011CrossRef Medline
22. Sheikh, I. A., and Beg, M. A. (2019) Structural characterization of potential endocrine disrupting activity of alternate plasticizers di-(2-ethylhexyl) adipate (DEHA), acetyl tributyl citrate (ATBC) and 2,2,4-trimethyl 1,3-pentanediol diisobutyrate (TPIB) with human sex hormone-binding globulin. *Reprod. Toxicol.* **83,** 46–53 CrossRef Medline
23. Sheikh, I. A., Tayubi, I. A., Ahmad, E., Ganaie, M. A., Bajouh, O. S., AlBasri, S. F., Abdulkarim, I. M. J., and Beg, M. A. (2017) Computational insights into the molecular interactions of environmental xenoestrogens 4-tert-octylphenol, 4-nonylphenol, bisphenol A (BPA), and BPA metabolite, 4-methyl-2, 4-bis (4-hydroxyphenyl) pent-1-ene (MBP) with human sex hormone-binding globulin. *Ecotoxicol. Environ. Saf.* **135,** 284–291 CrossRef Medline
24. Pohjoispää, M., and Wähälä, K. (2013) Synthesis of 3,4-dibenzyltetrahydrofuran lignans (9,9′-epoxylignanes). *Molecules* **18,** 13124–13138 CrossRef Medline
25. Minor, W., Cymborowski, M., Otwinowski, Z., and Chruszcz, M. (2006) HKL-3000: The integration of data reduction and structure solution—from diffraction images to an initial model in minutes. *Acta Crystallogr. D Biol. Crystallogr.* **62,** 859–866 CrossRef Medline
26. Kabsch, W. (2010) XDS. *Acta Crystallogr. D Biol. Crystallogr.* **66,** 125–132 CrossRef Medline
27. McCoy, A. J., Grosse-Kunstleve, R. W., Adams, P. D., Winn, M. D., Storoni, L. C., and Read, R. J. (2007) Phaser crystallographic software. *J. Appl. Crystallogr.* **40,** 658–674 CrossRef Medline
28. Emsley, P., Lohkamp, B., Scott, W. G., and Cowtan, K. (2010) Features and development of Coot. *Acta Crystallogr. D Biol. Crystallogr.* **66,** 486–501 CrossRef Medline
29. Adams, P. D., Afonine, P. V., Bunkóczi, G., Chen, V. B., Davis, I. W., Echols, N., Headd, J. J., Hung, L.-W., Kapral, G. J., Grosse-Kunstleve, R. W., McCoy, A. J., Moriarty, N. W., Oeffner, R., Read, R. J., Richardson, D. C., Richardson, J. S., Terwilliger, T. C., and Zwart, P. H. (2010) PHENIX: A comprehensive Python-based system for macromolecular structure solution. *Acta Crystallogr. D Biol. Crystallogr.* **66,** 213–221 CrossRef Medline
30. Jänne, M., Deol, H. K., Power, S. G., Yee, S. P., and Hammond, G. L. (1998) Human sex hormone-binding globulin gene expression in transgenic mice. *Mol. Endocrinol.* **12,** 123–136 CrossRef Medline
31. Campana, C., Rege, J., Turcu, A. F., Pezzi, V., Gomez-Sanchez, C. E., Robins, D. M., and Rainey, W. E. (2016) Development of a novel cell based androgen screening model. *J. Steroid Biochem. Mol. Biol.* **156,** 17–22 CrossRef Medline
32. Hammond, G. L., and Lähteenmäki, P. L. (1983) A versatile method for the determination of serum cortisol binding globulin and sex hormone binding globulin binding capacities. *Clin. Chim. Acta.* **132,** 101–110 CrossRef Medline

Molecular interactions between sex hormone–binding globulin and nonsteroidal ligands that enhance androgen activity

Phillip Round, Samir Das, Tsung-Sheng Wu, Kristiina Wähälä, Filip Van Petegem and Geoffrey L. Hammond

J. Biol. Chem. 2020, 295:1202-1211.
doi: 10.1074/jbc.RA119.011051 originally published online December 18, 2019
